This article has been accepted for publication in a future issue of this journal, but has not been fully edited. Content may change prior to final publication. Citation information: DOI 10.1109/TSG.2017.2709463, IEEE Transactions on Smart Grid

Fast Decoupled State Estimation for Distribution Networks Considering Branch Ampere Measurements

Yuntao Ju, *Member, IEEE,* Wenchuan Wu, *Senior Member*, Fuchao Ge, *Student Member*, Kang Ma, *Member, IEEE,* Yi Lin *and* Lin Ye, *Senior Member*

Abstract Fast decoupled state estimation (FDSE) is proposed for distribution networks, with fast convergence and high efficiency. Conventionally, branch current magnitude measurements cannot be incorporated into FDSE models; however, in this paper, branch ampere measurements are reformulated as active and reactive branch loss measurements and directly formulated in the proposed FDSE model. Using the complex per unit normalization technique and special chosen state variables, the performance of this FDSE can be guaranteed when it is applied to distribution networks. Numerical tests on seven different distribution networks show that this method outperforms Newton type solutions and is a promising method for practical application.

***Index Terms*—Distribution network, Fast decoupled state estimation, Ampere measurements**

NOMENCLATURE

$\vec{S}_{base}$	Complex power base
$\vec{I}_{base}$	Complex current base
S_{base}	Magnitude of complex power base
ϕ_{base}	Base angle, rad.
m	Number of branches
X_i	Reactance of branch i
R_i	Resistance of branch i
l	Number of PQ load
n	Number of state-undetermined buses
r	Number of slack buses
$\vec{U}_{base}$	Complex voltage base
U_{base}	Magnitude of complex voltage base
$\vec{Z}_{base}$	Complex impedance base
P_i	Active power injected at bus *i*
Q_i	Reactive power injected at bus *i*
α_{avg} , γ_{avg} , ε	Heuristic parameters calculated according to network parameters and load condition
$\boldsymbol{\theta}$	Phase angle vector with n dimension
$\boldsymbol{v}$	Voltage magnitude vector with n dimension
$\boldsymbol{x}$	State variables vector
$\boldsymbol{z}$	Measurements vector
$\boldsymbol{z}_a$	Active power measurements vector, include voltage phase angle measurements
$\boldsymbol{z}_r$	Reactive power measurements vector, include voltage magnitude measurements
$\boldsymbol{h}_a$	Calculated values responding to active power measurements
$\boldsymbol{h}_r$	Calculated values responding to reactive power measurements
$\boldsymbol{\varepsilon}_a$	Active power measurements error
$\boldsymbol{\varepsilon}_r$	Reactive power measurements error
$\boldsymbol{H}$	Measurement Jacobian
$\boldsymbol{R}^{-1}$	Weight matrix
$\boldsymbol{B}_a$	Constant measurement Jacobian matrix for active power measurements
$\boldsymbol{B}_r$	Constant measurement Jacobian matrix for reactive power measurements
I_{ij}^2	Square of branch current magnitude from bus i to bus j
$\boldsymbol{G}$	Gain matrix
$(\cdot)^m$	Measurements' value
μ	Average value
σ	Standard deviation

This work was supported partly by the National Science Foundation of China (Grant.51477083) ,the State Grid Fujian electric power company Economic institute of technology science and technology project (Grant SGFJJY00GHWT1600081) and the State Key Laboratory foundation project (Grant SKLD16KZ08).

Yuntao Ju and Lin Ye is with China Agricultural University, Beijing, China (e-mail: juyuntao@cau.edu.cn, yelin@cau.edu.cn).

Wenchuan Wu is with Tsinghua University, Beijing, China (corresponding author, email: wuwench@mail.tsinghua.edu.cn).

Yi Lin is with Fu Jian Electric Company (email: jyy.lin_yi@fj.sgcc.com.cn)

I. INTRODUCTION

STATE estimators (SEs) are significant data processors in electric power control centers (EPCCs), providing reliable information for real time markets [1]. Distribution system state estimation (DSE) is indispensable for active distribution network modeling and integrated operation with distributed energy resources [2].

Due to budget limitations, on many feeders, only branch current magnitude measurements (BCMMs) are deployed to

This article has been accepted for publication in a future issue of this journal, but has not been fully edited. Content may change prior to final publication. Citation information: DOI 10.1109/TSG.2017.2709463, IEEE Transactions on Smart Grid

monitor operating conditions. Some investigations have shown that these real-time BCMMs can significantly improve the accuracy of load estimation in DSE [3]. However, BCMMs are usually ignored in transmission SE due to their coupled property and mathematical problems [4], such as zero elements in the measurement Jacobian evaluated at flat start and multiple solutions [5].

In DSE, BCMMs are usually handled indirectly. In [3], a strategy with two stages is proposed. In the first stage, the branch current measurements are disregarded. In the second stage, the BCMMs are approximately formulated as linear complex measurements, with the phase angle estimated in the first stage, and the updated SE model is iteratively solved. In [6], BCCMs, and active and reactive power measurements, are all transformed to linear complex current measurements based on estimated phase angle and voltage. Clearly, these solutions will introduce additional errors due to measurement transformation.

BCCMs can be directly formulated in DSE with special selection of state variables. A branch current-based DSE is proposed to accommodate large-scale BCCMs, where the magnitude and phase angle of the branch current were selected as the state variables in [7]. Another formulation of DSE adopts branch current magnitude and power as state variables [8]. However, these methods suffer from a heavy computational burden for large-scale networks, because repeated factorization of the gain matrix is involved.

Fast decoupled state estimation (FDSE) algorithms are used widely for transmission networks [9], [10] [11] due to their high efficiency. FDSE has become a standard method for SE in energy management systems (EMSs) [12].

Numerical tests on variable transmission networks indicate that the gain matrix of SE changes slightly during the iteration procedure [9]. Under certain assumptions, a constant gain matrix in a decoupled pattern can be obtained. The right hand side (RHS) of normal equations can also be decoupled [10]. Ill-conditioned problems of SE occur when there are small impedance branches [13], weights that are too large for virtual zero injection measurements, etc. These problems can be addressed by normal equations with constraints [14] [15] or Hachtel's augmented matrix method [16]. A fast decoupled formulation for SE based on Hachtel's sparse tableaux approach is proposed in [12]. To improve the numerical stability of FDSE, an orthogonal row processing algorithm can be used with Givens transformations. [17]. Because the orthogonal transformation needs to store a dense and high dimension transformation matrix, it is computationally complex and not highly practical. Decoupled SE can also be carried out in rectangular form via transformation of active and reactive measurement pairs to linear complex current measurements [18]. FDSE shows bad convergence performance for networks with high r/x ratios. Therefore, a new FDSE is required, maintaining nonzero coupling in the Jacobian off-diagonal matrix block in an iterative procedure to improve performance under high r/x ratios [19].

Several practical solutions have been developed to resolve the problem in FDSE of high r/x ratios in a distribution network. A rotation-based method has been presented to handle this difficulty [20]. O. L. Tortelli et al. propose a fast decoupled algorithm via complex *pu* normalization [21] for distribution networks.

In summary, to the best of our knowledge, with the complex *pu* technique, FDSE can be implemented on distribution networks with promising convergence; however, incorporation of BCCMs in an FDSE model remains a problem requiring a solution. In a typical distribution network, branch current measurements represent the major portion of their limited real-time measurements. In this paper, a novel fast decoupled distribution state estimator (FD-DSE) is proposed. The branch ampere measurements are equivalently reformulated as the branch active power and reactive power losses, and the power loss measurements can be incorporated into the FD-DSE model in a decoupled manner. Numerical tests show that this FD-DSE has a low computational burden with fast convergence.

II. Brief Review of Fast Decoupled State Estimation

By introducing the complex per unit normalization [21], normalized r/x ratio of distribution network becomes smaller, a fast decoupled algorithm can be realized with robust performance. The main concept underlying complex per unit normalization is explained briefly here.

A. Complex per unit Normalization

First, a complex volt-ampere base is given by:

$$\vec{S}_{base} = \left|\vec{S}_{base}\right| \cdot e^{-j\phi_{base}}, \tag{1}$$

where $\vec{S}_{base}$ denotes complex power base, S_{base} denotes magnitude of complex power base, ϕ_{base} denotes angle base.

The voltage base is given by:

$$\vec{U}_{base} = U_{base} + j0, \tag{2}$$

where $\vec{U}_{base}$ denotes complex voltage base, $\vec{U}_{base}$ denotes magnitude of complex voltage base.

According to (1) and (2), the current and impedance base will be:

$$\vec{Z}_{base} = \frac{U_{base}^2}{\vec{S}_{base}^*} = \left|\frac{U_{base}^2}{S_{base}}\right| e^{-j\phi_{base}} \tag{3}$$

$$\vec{I}_{base} = \frac{\vec{S}_{base}^*}{U_{base}} = \left|\frac{S_{base}}{U_{base}}\right| e^{j\phi_{base}} \tag{4}$$

where $\vec{I}_{base}$ denotes complex current base, $\vec{Z}_{base}$ denotes complex impedance base.

The determination of the base angle is achieved by:

$$\phi_{base} = \left(\frac{\pi}{2} - \frac{\alpha_{avg} + \gamma_{avg}}{2}\right)(1+\varepsilon) \tag{5}$$

where

$$\alpha_{avg} = \frac{\sum_{i=1}^{m} \tan^{-1}\left(\frac{X_i}{R_i}\right)}{m},$$

$$\gamma_{avg} = \frac{\tan^{-1}\left(\frac{X_i}{R_i}\right)_{\max} + \tan^{-1}\left(\frac{X_i}{R_i}\right)_{\min}}{2},$$

$$\varepsilon = 1 - \frac{\sum_{i=1}^{l} \cos\left(\tan^{-1}\left(\frac{Q_i}{P_i}\right)\right)}{l},$$

where m denotes the number of branches, X_i and R_i are the reactance and resistance of branch i, l is the number of PQ

This article has been accepted for publication in a future issue of this journal, but has not been fully edited. Content may change prior to final publication. Citation information: DOI 10.1109/TSG.2017.2709463, IEEE Transactions on Smart Grid

load, P_i and Q_i are active and reactive power injected at bus *i*, α_{avg}, γ_{avg}, ε are heuristic parameters calculated according to network parameters and load conditions.

With the above-mentioned complex per unit normalization, the normalized r/x ratio of a distribution becomes smaller; a fast-decoupled algorithm can be used for distribution networks.

B. Fast Decoupled State Estimation

For an electrical power network, the state variables are composed of phase angle $\boldsymbol{\theta}$ and voltage magnitude $\boldsymbol{v}$.

The objective of the weighted least squares SE model is:

$$\min \sum_{i\in\Phi_m} R_i^{-1}(z_i - h_i(\mathrm{x}))^2 \tag{6}$$

where $x=\{v_i,\theta_i\}$.

This SE problem can be solved using the Newton method, and the iterative equation is [1]:

$$\Delta \boldsymbol{x} = \boldsymbol{G}^{-1}\boldsymbol{H}^T\boldsymbol{R}^{-1}(\boldsymbol{z}-\boldsymbol{h}(\boldsymbol{x})) \tag{7}$$

where $\boldsymbol{G}=\boldsymbol{H}^T\boldsymbol{R}\boldsymbol{H}$, $\boldsymbol{H}=\dfrac{\partial \boldsymbol{h}(\boldsymbol{x})}{\partial \boldsymbol{x}}$.

The measurement vector can be divided into active and reactive power parts:

$$\boldsymbol{z}=\begin{bmatrix}\boldsymbol{z}_a\\ \boldsymbol{z}_r\end{bmatrix}=\begin{bmatrix}\boldsymbol{h}_a\ \ \boldsymbol{\theta},\boldsymbol{v}\\ \boldsymbol{h}_r\ \ \boldsymbol{\theta},\boldsymbol{v}\end{bmatrix}+\begin{bmatrix}\boldsymbol{\varepsilon}_a\\ \boldsymbol{\varepsilon}_r\end{bmatrix} \tag{8}$$

The measurement Jacobian matrix can be divided into two parts and is written as:

$$\boldsymbol{H}=\begin{bmatrix}\dfrac{\partial \boldsymbol{h}_a}{\partial \boldsymbol{\theta}} & \dfrac{\partial \boldsymbol{h}_a}{\partial \boldsymbol{v}}\\ \dfrac{\partial \boldsymbol{h}_r}{\partial \boldsymbol{\theta}} & \dfrac{\partial \boldsymbol{h}_r}{\partial \boldsymbol{v}}\end{bmatrix}=\begin{bmatrix}\boldsymbol{H}_{aa} & \boldsymbol{H}_{ar}\\ \boldsymbol{H}_{ra} & \boldsymbol{H}_{rr}\end{bmatrix} \tag{9}$$

The weight matrix $\boldsymbol{R}^{-1}$ can also be divided into two parts:

$$\boldsymbol{R}^{-1}=\begin{bmatrix}\boldsymbol{R}_a^{-1} & \\ & \boldsymbol{R}_r^{-1}\end{bmatrix} \tag{10}$$

Considering that $\dfrac{\partial \boldsymbol{h}_a}{\partial \boldsymbol{v}}\approx 0$, $\dfrac{\partial \boldsymbol{h}_r}{\partial \boldsymbol{\theta}}\approx 0$ after complex per unit normalization, and assuming that $\theta_{ij}\approx 0, v_i\approx 1$, the gain matrix is expressed by:

$$\frac{\partial \boldsymbol{h}_a}{\partial \boldsymbol{\theta}}=-\boldsymbol{B}_a \tag{11}$$

$$\frac{\partial \boldsymbol{h}_r}{\partial \boldsymbol{v}}=-\boldsymbol{B}_r \tag{12}$$

According to the proposition of fast decoupled power flow [22], $\boldsymbol{B}_a$ is formulated with $-\dfrac{1}{x_b}$, where x_b is the branch reactance and $\boldsymbol{B}_r$ is formulated with the imaginary part of the branch admittance.

Finally, the FDSE is formulated with two incremental equations. First, the phase angles are corrected using:

$$\boldsymbol{B}_a^T\boldsymbol{R}_a^{-1}\boldsymbol{B}_a\Delta\boldsymbol{\theta}=-\boldsymbol{B}_a^T\boldsymbol{R}_a^{-1}\left[\boldsymbol{z}_a-\boldsymbol{h}_a\ \ \boldsymbol{v},\boldsymbol{\theta}\right] \tag{13}$$

Then, the voltage magnitudes are corrected using:

$$\boldsymbol{B}_r^T\boldsymbol{R}_r^{-1}\boldsymbol{B}_r\Delta\boldsymbol{v}=-\boldsymbol{B}_r^T\boldsymbol{R}_r^{-1}\left[\boldsymbol{z}_r-\boldsymbol{h}_r\ \ \boldsymbol{v},\boldsymbol{\theta}\right] \tag{14}$$

Because of its high efficiency and low memory cost, FDSE with (13) and (14) has become a standard algorithm in EMSs.

C. Difficulties in Accounting for Branch Current Magnitude Measurements in FDSE

The branch current can be expressed as [23]:

$$I_{ij}^2=\left(g_{ij}^2+b_{ij}^2\right)\left(v_i^2+v_j^2-2v_iv_j\cos\theta_{ij}\right) \tag{15}$$

The measurement Jacobian for the square of BCCM is given by:

$$\frac{\partial I_{ij}^2}{\partial v_i}=2\left(g_{ij}^2+b_{ij}^2\right)\left(v_i-v_j\cos\theta_{ij}\right) \tag{16}$$

$$\frac{\partial I_{ij}^2}{\partial \theta_i}=2\left(g_{ij}^2+b_{ij}^2\right)v_iv_j\sin\theta_{ij} \tag{17}$$

For flat start, assume that $v_i\approx v_j\approx 1$, $\theta_i\approx\theta_j$, (16) and (17) are both equal to zero and are useless at flat start. Reference [23] concludes that BCMM cannot be decoupled or used in FDSE. Since BCMMs occupy a large portion of real-time measurements in distribution networks, they should be exploited thoroughly in DSE.

III. Proposed Distribution State Estimation Model

The voltage vector ($v_i\angle\theta_i$), and real and reactive branch power flow (P_{ij}, Q_{ij}, P_{ji}, Q_{ji}) are selected as state variables. Therefore, there are $4m$ additional state variables compared with the conventional SE model. Let $\boldsymbol{z}$ represent the measurement vector, and R_i^{-1} the weight of the *i*th measurement

The measurement equation $h(\boldsymbol{y})$ relating the measurement vector and the state vector includes:

1) Real and reactive power measurements of the branch:

$$\left(P_{ij}\right)^m=P_{ij}+\varepsilon_{P_{ij}},\ \left(Q_{ij}\right)^m=Q_{ij}+\varepsilon_{P_{ij}} \tag{18}$$

where ε represents the measurement error, and the superscript m denotes measurement quantities.

2) Injection power measurements:

$$\left(P_i\right)^m=\sum_{j\in i}P_{ij}+\varepsilon_{P_i},\ \left(Q_i\right)^m=\sum_{j\in i}Q_{ij}-Q_{i,cap}+\varepsilon_{Q_i} \tag{19}$$

where $j\in i$ denotes that j is connected to i and $Q_{i,cap}$ is reactive power injected by capacitors.

3) Branch current measurements:

$$I_{ij}^{m2}r_{ij}=P_{ij,loss}^m=P_{ij}+P_{ji}+\varepsilon_{P_{ij,loss}} \tag{20}$$

$$I_{ij}^{m2}x_{ij}=Q_{ij,loss}^m=Q_{ij}+Q_{ji}-v_i^2b_{sh,ij}-v_j^2b_{sh,ij}+\varepsilon_{Q_{ij,loss}} \tag{21}$$

where $b_{sh,ij}$ is the 1/2 branch charging susceptance. I_{ij}^m denotes a branch current measurement, and subscript *loss* denotes branch loss. Since the branch charging current for a distribution network is very small, these two approximate equations have only trivial errors.

When BCCMs are the only ones to make the branch observable, the SE solution is not unique [23](chapter 9). It means BCCMs cannot be critical measurements to make the branch observable, i.e. BCCMs are redundant measurements to make SE more accurate.

4) Bus voltage measurements:

This article has been accepted for publication in a future issue of this journal, but has not been fully edited. Content may change prior to final publication. Citation information: DOI 10.1109/TSG.2017.2709463, IEEE Transactions on Smart Grid

$$(v_i)^m = v_i + \varepsilon_{U_i} \tag{22}$$

5) Virtual measurements:

Because $4m$ additional state variables have been introduced into state estimation, $4m$ extra constraints should be supplemented, as virtual measurements, to insure the observability of the system.

For a branch, the branch active and reactive power constraints can be formulated as virtual measurements and expressed as:

$$f_{p,v} = P_{ij} - v_i \frac{r_{ij}\left(v_i - v_j\cos\left(\theta_i-\theta_j\right)\right) + x_{ij}v_j\sin\left(\theta_i-\theta_j\right)}{\left(r_{ij}^2 + x_{ij}^2\right)} = 0 \tag{23}$$

$$f_{q,v} = Q_{ij} - v_i \frac{x_{ij}\left(v_i - v_j\cos\left(\theta_i-\theta_j\right)\right) + r_{ij}v_j\sin\left(\theta_i-\theta_j\right)}{\left(r_{ij}^2 + x_{ij}^2\right)} = 0 \tag{24}$$

Similar constraints can be derived for P_{ji} and Q_{ji} flow from the other side of the branch. Effects of charging susceptance are neglected in (23) and (24).

For shunt capacitors, the branch power flow constraints are formulated as:

$$Q_{i,cap} - v_i^2 b_{i,cap} = 0 \tag{25}$$

where $b_{i,cap}$ is the susceptance of capacitors.

The whole measurement Jacobian is expressed as $\boldsymbol{H}$, where

$$\boldsymbol{H} = \begin{bmatrix}
\boldsymbol{\theta} & \boldsymbol{v} & \boldsymbol{P}_{ij} & \boldsymbol{P}_{ji} & \boldsymbol{Q}_{ij} & \boldsymbol{Q}_{ji} \\
0 & 0 & \frac{\partial \boldsymbol{P}_{inj}}{\partial \boldsymbol{P}_{ij}} & \frac{\partial \boldsymbol{P}_{inj}}{\partial \boldsymbol{P}_{ji}} & 0 & 0 \\
0 & 0 & 0 & 0 & \frac{\partial \boldsymbol{Q}_{inj}}{\partial \boldsymbol{Q}_{ij}} & \frac{\partial \boldsymbol{Q}_{inj}}{\partial \boldsymbol{Q}_{ji}} \\
0 & 0 & \frac{\partial \boldsymbol{P}_{flow}}{\partial \boldsymbol{P}_{ij}} & \frac{\partial \boldsymbol{P}_{flow}}{\partial \boldsymbol{P}_{ji}} & 0 & 0 \\
0 & 0 & 0 & 0 & \frac{\partial \boldsymbol{Q}_{flow}}{\partial \boldsymbol{Q}_{ij}} & \frac{\partial \boldsymbol{Q}_{fllow}}{\partial \boldsymbol{Q}_{ji}} \\
0 & 0 & \frac{\partial \boldsymbol{P}_{loss}}{\partial \boldsymbol{P}_{ij}} & \frac{\partial \boldsymbol{P}_{loss}}{\partial \boldsymbol{P}_{ji}} & 0 & 0 \\
0 & 0 & 0 & 0 & \frac{\partial \boldsymbol{Q}_{loss}}{\partial \boldsymbol{Q}_{ij}} & \frac{\partial \boldsymbol{Q}_{loss}}{\partial \boldsymbol{Q}_{ji}} \\
\frac{\partial \boldsymbol{f}_{p,v}}{\partial \boldsymbol{\theta}} & \frac{\partial \boldsymbol{f}_{p,v}}{\partial \boldsymbol{v}} & \frac{\partial \boldsymbol{f}_{p,v}}{\partial \boldsymbol{P}_{ij}} & \frac{\partial \boldsymbol{f}_{p,v}}{\partial \boldsymbol{P}_{ji}} & 0 & 0 \\
\frac{\partial \boldsymbol{f}_{q,v}}{\partial \boldsymbol{\theta}} & \frac{\partial \boldsymbol{f}_{q,v}}{\partial \boldsymbol{v}} & 0 & 0 & \frac{\partial \boldsymbol{f}_{q,v}}{\partial \boldsymbol{Q}_{ij}} & \frac{\partial \boldsymbol{f}_{q,v}}{\partial \boldsymbol{Q}_{ji}} \\
0 & \frac{\partial \boldsymbol{V}_{mag}}{\partial \boldsymbol{v}} & 0 & 0 & 0 & 0
\end{bmatrix},$$

where $\boldsymbol{P}_{flow}, \boldsymbol{Q}_{flow}$ represent active and reactive power flow measurements vectors, $\boldsymbol{P}_{loss}, \boldsymbol{Q}_{loss}$ represent active and reactive branch power loss measurements' vectors, $\boldsymbol{P}_{inj}, \boldsymbol{Q}_{inj}$ represent active and reactive power injection measurements' vectors, $\boldsymbol{f}_{p,v}, \boldsymbol{f}_{q,v}$ represent virtual measurements provided by branch constraints in equation (23) and equation (24), $\boldsymbol{P}_{ij}, \boldsymbol{P}_{ji}, \boldsymbol{Q}_{ij}, \boldsymbol{Q}_{ji}$ represent additional real and reactive branch power flow as additional state variables. $\boldsymbol{V}_{mag}$ represents voltage magnitude measurements.

The corresponding elements of matrix $\boldsymbol{H}$ are described as:

$\frac{\partial P_i}{\partial P_{ij}} = 1$, $\frac{\partial Q_i}{\partial Q_{ij}} = 1$, $\frac{\partial P_{ij}}{\partial P_{ij}} = 1$, $\frac{\partial Q_{ij}}{\partial Q_{ij}} = 1$, $\frac{\partial P_{ij,loss}}{\partial P_{ij}} = 1$, $\frac{\partial P_{ij,loss}}{\partial P_{ji}} = 1$,

$\frac{\partial Q_{loss}}{\partial Q_{ji}} = 1$, $\frac{\partial Q_{loss}}{\partial Q_{ij}} = 1$, $\frac{\partial f_{ij,p,v}}{\partial P_{ij}} = 1$,

$\frac{\partial f_{ij,p,v}}{\partial v_i} = -\left(2v_i g - v_j g\cos\theta_{ij} - v_j b\sin\theta_{ij}\right)$,

$\frac{\partial f_{ij,p,v}}{\partial \theta_i} = -v_i v_j\left(g\sin\theta_{ij} - b\cos\theta_{ij}\right)$,

$\frac{\partial f_{ij,p,v}}{\partial v_j} = v_i\left(g\cos\theta_{ij} + b\sin\theta_{ij}\right)$,

$\frac{\partial f_{ij,p,v}}{\partial \theta_j} = v_i v_j\left(g\sin\theta_{ij} - b\cos\theta_{ij}\right)$,

$\frac{\partial f_{ij,q,v}}{\partial Q_{ij}} = 1$, $\frac{\partial f_{ij,q,v}}{\partial v_i} = 2v_i\left(b + y_c\right) + v_j\left(g\sin\theta_{ij} - b\cos\theta_{ij}\right)$,

$\frac{\partial f_{ij,q,v}}{\partial \theta_i} = v_i v_j\left(g\cos\theta_{ij} + b\sin\theta_{ij}\right)$,

$\frac{\partial f_{ij,q,v}}{\partial v_j} = v_i\left(g\sin\theta_{ij} - b\cos\theta_{ij}\right)$,

$\frac{\partial f_{ij,q,v}}{\partial \theta_j} = -v_i v_j\left(g\cos\theta_{ij} + b\cos\theta_{ij}\right)$, $\frac{\partial V_i}{\partial v_i} = 1$. Here g and b denote branch admittance, y_c denotes shunt susceptance.

It shows that no elements are faced with zero problem under the assumption $\theta_{ij} \approx 0$. So, the proposed measurement model can cope with branch currents model in a decoupled manner.

FDSE depends on the PQ decoupled properties of the measurement equations. Branch power measurements (18), injection power measurements (19) and branch loss measurements (20)(21)(25) all have PQ decoupled properties; however, the virtual branch constraints (23)(24) are involved in both v and θ. It has been observed that v has little impact on active power and that θ has little impact on reactive power for a distribution network with high R/X in a complex per unit system [21], and that $\sin\left(\theta_i - \theta_j\right) \approx \theta_i - \theta_j$, $\cos\left(\theta_i - \theta_j\right) \approx 1$, and $v_j \approx 1$. Therefore, according to the proposition from fast decoupled power flow, the elements of the measurement Jacobian for the virtual branch constraints of (23)(24) can be formulated as:

$$\frac{\Delta P_{ij}}{v_i} \approx \frac{\left(\Delta\theta_i - \Delta\theta_j\right)}{x_{ij}} \tag{26}$$

$$\frac{\Delta Q_{ij}}{v_i} = -\frac{x_{ij}\left(\Delta v_i - \Delta v_j\right)}{\left(r_{ij}^2 + x_{ij}^2\right)} \tag{27}$$

This article has been accepted for publication in a future issue of this journal, but has not been fully edited. Content may change prior to final publication. Citation information: DOI 10.1109/TSG.2017.2709463, IEEE Transactions on Smart Grid

For FD-DSE, the measurement jacobian matrix is expressed in equation (9), where $\boldsymbol{H}_{ar}$ =0, $\boldsymbol{H}_{ra}$ =0, and the other two matrixes are

$$\boldsymbol{H}_{aa}=\begin{array}{c} \begin{matrix} \theta & \boldsymbol{P}_{ij} & \boldsymbol{P}_{ji} \end{matrix} \\ \begin{bmatrix} 0 & \frac{\partial \boldsymbol{P}_{inj}}{\partial \boldsymbol{P}_{ij}} & \frac{\partial \boldsymbol{P}_{inj}}{\partial \boldsymbol{P}_{ji}} \\ 0 & \frac{\partial \boldsymbol{P}_{flow}}{\partial \boldsymbol{P}_{ij}} & \frac{\partial \boldsymbol{P}_{flow}}{\partial \boldsymbol{P}_{ji}} \\ 0 & \frac{\partial \boldsymbol{P}_{loss}}{\partial \mathrm{P}_{ij}} & \frac{\partial \boldsymbol{P}_{loss}}{\partial \mathrm{P}_{ji}} \\ \frac{\partial \boldsymbol{f}_{p,v}}{\partial \theta} & \frac{\partial \boldsymbol{f}_{p,v}}{\partial \boldsymbol{P}_{ij}} & \frac{\partial \boldsymbol{f}_{p,v}}{\partial \boldsymbol{P}_{ji}} \end{bmatrix} \end{array},$$

$$\boldsymbol{H}_{rr}=\begin{array}{c} \begin{matrix} v & \boldsymbol{Q}_{ij} & \boldsymbol{Q}_{ji} \end{matrix} \\ \begin{bmatrix} 0 & \frac{\partial \boldsymbol{Q}_{inj}}{\partial Q_{ij}} & \frac{\partial \boldsymbol{Q}_{inj}}{\partial \boldsymbol{Q}_{ji}} \\ 0 & \frac{\partial \boldsymbol{Q}_{flow}}{\partial \boldsymbol{Q}_{ij}} & \frac{\partial \boldsymbol{Q}_{flow}}{\partial \boldsymbol{Q}_{ji}} \\ 0 & \frac{\partial \boldsymbol{Q}_{loss}}{\partial \boldsymbol{Q}_{ij}} & \frac{\partial \boldsymbol{Q}_{loss}}{\partial \boldsymbol{Q}_{ji}} \\ \frac{\partial \boldsymbol{f}_{q,v}}{\partial v} & \frac{\partial \boldsymbol{f}_{q,v}}{\partial \boldsymbol{Q}_{ij}} & \frac{\partial \boldsymbol{f}_{q,v}}{\partial \boldsymbol{Q}_{ji}} \\ \frac{\partial \boldsymbol{V}_{mag}}{\partial v} & 0 & 0 \end{bmatrix} \end{array}.$$

The corresponding elements of matrix $\boldsymbol{H}_{aa}$ and $\boldsymbol{H}_{rr}$ are described as:

$$\frac{\partial Q_i}{\partial Q_{ij}}=1,\ \frac{\partial Q_{ij}}{\partial Q_{ij}}=1,\ \frac{\partial Q_{ji,loss}}{\partial Q_{ji}}=1,\ \frac{\partial f_{ij,q,v}}{\partial Q_{ij}}=1,\ \frac{\partial V_i}{\partial v_i}=1$$

$$\frac{\partial P_i}{\partial P_{ij}}=1,\frac{\partial P_{ij}}{\partial P_{ij}}=1,\ \frac{\partial P_{ij,loss}}{\partial P_{ij}}=1,\frac{\partial P_{ij,loss}}{\partial P_{ji}}=1.$$

The Jacobian matrix entries keep constant during the iteration. Every nonlinear entries are approximated with $\frac{\partial f_{ij,p,v}}{\partial \theta_i}\approx\frac{1}{x_{ij}}$, $\frac{\partial f_{ij,q,v}}{\partial v_i}\approx\frac{x_{ij}}{r_{ij}^2+x_{ij}^2}$, according to fast decoupled power flow solution proposed in[22]. Other elements are either 1 or 0.

The element of the measurement Jacobian for the shunt capacitor is:

$$\frac{\Delta Q_{i,cap}}{v_i}=b_{i,cap} \tag{28}$$

By adopting the above measurement Jacobian formulation scheme, a fast decoupled distribution SE (FD-DSE) can be formulated, in which the two Jacobian matrixes for the *P-θ* and *Q-V* iterations are both constant. The calculation procedure for the FD-DSE is similar to the FDSE introduced in (13) and (14) [23]. The whole FD-DSE flow chart is depicted in Fig. 1.

The usage of complex pu normalization in a state estimation problem includes three steps:

(1)The key for complex pu normalization method is to estimate the base angle ϕ_{base}, according to equation (5), this value is mainly determined by network parameters and load factor. In distribution network, load factor can be estimated according to load type.

(2)Calculate complex volt-ampere base, impedance base and current base according to the estimated base angle ϕ_{base}.

(3)All measurements and network parameters are normalized according to the base values using complex pu normalization.

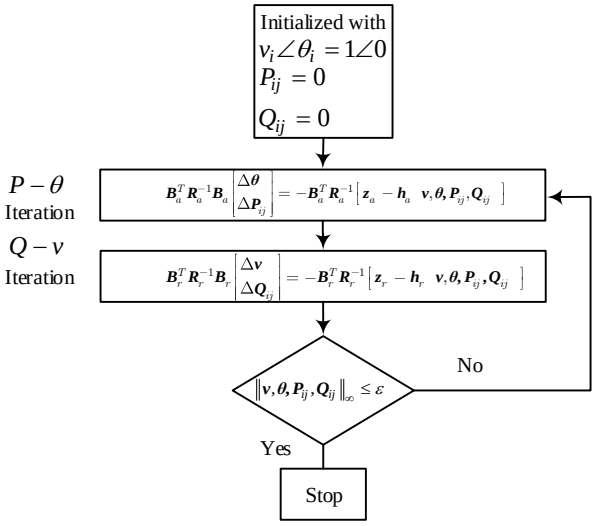

Figure 1 Flowchart of the whole fast decoupled distribution state estimator (FD-DSE)

Discussion on its observability: For a distribution network with m branches, 4m additional state variables are involved in this SE model, and branch constraints (23)(24) can provide a total of 4m extra equations in the same time. Therefore, the proposed SE model has the same observability as a conventional SE. Because the dimensions of $\boldsymbol{B}_a$ and $\boldsymbol{B}_r$ being larger than those of the conventional SE is not very important for sparse matrices [14], the proposed FDSE has promising computational performance for practical applications.

IV. Bad Data Analysis

Chi-squares test is used for detecting bad data [23]. Normalized residuals are usually used for bad data identification [32]. Hypothesis testing identification (HTI) can be used for identifying multiple errors [33]. In proposed FD-DSE, HTI is used to identify bad data and the analysis procedure is described as followings:

(1)suspect measurement set s is selected according to normalized residuals r^N and calculate $\hat{e}_s=S_{ss}^{-1}\left(z-\hat{z}\right)$,where S_{ss} represents residual sensitivity matrix corresponding to suspect measurement set. $\hat{z}$ denotes estimated measurements value and z denotes measurements' value.

This article has been accepted for publication in a future issue of this journal, but has not been fully edited. Content may change prior to final publication. Citation information: DOI 10.1109/TSG.2017.2709463, IEEE Transactions on Smart Grid

(2)Calculate $N_{\left(1-\frac{\alpha}{2}\right)i}=\dfrac{\left|e_{si}\right|+\sigma_i N_\beta\sqrt{T_{ii}-1}}{\sigma_i\sqrt{T_{ii}}}$, where $T=S_{ss}^{-1}$, σ_i^2 variance, α denotes the probability of making an error in rejection of valid measurements, $N_\beta=b$,(for example, $b=-2.32$ for $\beta=0.01$).

(3)If $0\le N_{\left(1-\frac{\alpha}{2}\right)i}\le N_{\left(1-\frac{\alpha}{2}\right)\max}$, $\lambda_i=\sigma_i\sqrt{T_{ii}}N_{\left(1-\frac{\alpha}{2}\right)i}$, where $N_{\left(1-\frac{\alpha}{2}\right)\max}=3.0$ .If $N_{\left(1-\frac{\alpha}{2}\right)i}<0$, $\lambda_i=\sigma_i\sqrt{T_{ii}}N_{\left(1-\frac{\alpha}{2}\right)i\max}$ .If $N_{\left(1-\frac{\alpha}{2}\right)i}>N_{\left(1-\frac{\alpha}{2}\right)\max}$, $\lambda_i=\sigma_i\sqrt{T_{ii}}N_{\left(1-\frac{\alpha}{2}\right)i\max}$.

(4)Taken as suspect measurements if $\left|e_{si}\right|>\lambda_i$.

(5)Repeat steps 1-4 until all measurements that are suspected in the previous iteration are all selected again at step 4. Bad data identification algorithm can be accelerated using algorithm in [35].

The detail of HTI based bad data identification can refer to [23] and [32].

V. Simple Illustrative Sample

To explain the procedure of the proposed method more clearly, the FD-DSE is implemented on a simple two-bus sample network.

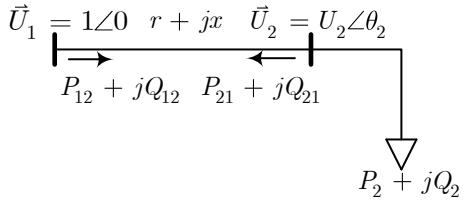

Figure 2 Two-bus illustrative sample system

The original impedance, and active and reactive power under a conventional per unit system, are $r+jx = 0.0967 + 0.0397$j p.u. and $P_2 + jQ_2 = 0.0042 + 0.0026$j. According to (5), the base angle for complex per unit normalization can be obtained as $\phi_{base}=1.3581$ rad. Then, by implementing complex unit normalization on this simple two-bus system, measurements can be generated with original power flow adding errors, which satisfy a Gaussian distribution. The measurement parameters for the Gaussian distribution are given in Table I.

TABLE I
Parameters for Distributions of Measurements

Measurement	μ	σ
P_2	-1.6548e-3	1.656e-9
Q_2	4.6542e-3	4.655e-9
Square BCCM of branch 1-2	0.17997	1.7997e-7
Active power loss of branch 1-2	-0.003310	3.31e-9
Reactive power loss of branch 1-2	0.009311	9.31e-9

Then, the active power injection measurements are given by:

$$P_2^m=P_{21}+\varepsilon_{a,1} \tag{29}$$

$$Q_2^m=Q_{21}+\varepsilon_{r,1} \tag{30}$$

The equations for the virtual measurements are expressed as:

$$0=P_{12}-\frac{v_1 r\left(v_1-v_1\cos\left(\theta_1-\theta_2\right)\right)+v_1 x v_2\sin\left(\theta_1-\theta_2\right)}{\left(r^2+x^2\right)} \tag{31}$$

$$0=P_{21}-\frac{v_2 r\left(v_2-v_2\cos\left(\theta_2-\theta_1\right)\right)+v_2 x v_1\sin\left(\theta_2-\theta_1\right)}{\left(r^2+x^2\right)} \tag{32}$$

$$0=Q_{12}-\frac{v_1 x\left(v_1-v_2\cos\left(\theta_1-\theta_2\right)\right)+v_1 r v_2\sin\left(\theta_1-\theta_2\right)}{\left(r^2+x^2\right)} \tag{33}$$

$$0=Q_{21}-\frac{v_2 x\left(v_1-v_1\cos\left(\theta_2-\theta_1\right)\right)+v_2 r v_1\sin\left(\theta_2-\theta_1\right)}{\left(r^2+x^2\right)} \tag{34}$$

The power loss measurements are given by:

$$P_{loss}^m=P_{12}+P_{21} \tag{35}$$

$$Q_{loss}^m=Q_{12}+Q_{21} \tag{36}$$

Since all the measurements satisfy PQ decoupled characteristics, matrix $\boldsymbol{B}_a$ is given by:

$$\boldsymbol{B}_a=\begin{array}{c}\\ P_2^m\\ 0^m\\ 0^m\\ P_{loss}^m\end{array}\begin{array}{c}\begin{array}{ccc}\theta_2 & P_{12} & P_{21}\end{array}\\ \begin{bmatrix}0 & 0 & 1\\ 1/x & 1 & 0\\ -1/x & 0 & 1\\ 0 & 1 & 1\end{bmatrix}\end{array} \tag{37}$$

Similar to the active power part, $\boldsymbol{B}_r$ is formulated as:

$$\boldsymbol{B}_r=\begin{array}{c}\\ Q_2^m\\ 0^m\\ 0^m\\ Q_{loss}^m\end{array}\begin{array}{c}\begin{array}{ccc}v_2 & Q_{12} & Q_{21}\end{array}\\ \begin{bmatrix}0 & 0 & 1\\ x/\left(r^2+x^2\right) & 1 & 0\\ -x/\left(r^2+x^2\right) & 0 & 1\\ 0 & 1 & 1\end{bmatrix}\end{array} \tag{38}$$

Then, according to (13) and (14), this SE model can be solved in a decoupled manner. The FD-DSE for this simple illustrative sample network converged after three iterations.

It can be seen that $\boldsymbol{B}_a$ and $\boldsymbol{B}_r$ have zero pivot in lower-upper triangular (LU) decomposition, which can be accounted for easily with an MC64 pivoting algorithm [24] to ensure the numerical stability of the FD-DSE.

VI. Test Cases

The FD-DSE was programmed in C++ and tested on several practical or hypothetical radial and meshed distribution networks [25]. Six cases on radial or meshed networks, with all branches deployed with BCCMs and all loads equipped with active and reactive power measurements, were designed for testing. The average values for all measurements were the original power flow values. The measurement errors satisfy a Gaussian distribution, with standard deviations given by

$$\sigma=10^{-6}z_{pf}+10^{-12} \tag{39}$$

where z_{pf} denotes the power flow result for this measurement.

(1) Case 1: 29-bus test feeder, with 1 reference bus and 1 tie branch [26];

(2) Case 2: 32-bus test feeder, with 1 reference bus and 5 tie

This article has been accepted for publication in a future issue of this journal, but has not been fully edited. Content may change prior to final publication. Citation information: DOI 10.1109/TSG.2017.2709463, IEEE Transactions on Smart Grid

branches [27];

(3) Case 3: 83-bus test feeder, with 11 reference buses and 13 tie branches [28];

(4) Case 4: 135-bus test feeder, with 8 reference buses and 21 tie branches [25];

(5) Case 5: 201-bus test feeder, with 3 reference buses and 15 tie branches [25];

(6) Case 6: 873-bus test feeder, with 7 reference buses and 27 tie branches [25];

(7) Case 7: 10476-bus test feeder, with 84 reference buses and 260 tie branches [25];

The programs were compiled using "**g++ -o0 –g3 –Wall –c –MMD –MP -MF**" on a Fedora 25 Linux operating system and executed on a notebook PC (ThinkPad X1Carbon; 2.3-GHz CPU). The functions and operations on dense and sparse matrices were developed based on the Armadillo [29], Eigen [30] and SuperLab [31] open source codes.

A. Performance Comparison with Newton Base SE

From numerical test cases 1-7, with only deploying critical measurements, the results show that proposed method and traditional SE can both obtain SE results. These tests verify that the proposed SE model has the same observability as a conventional SE.

The test results of the FD-DSE and Newton-DSE are listed in Table II and Table III, with an average value of 100 Monte Carlo simulations and where "Iter." denotes the number of iterations. Table II lists the results for radial networks, while Table III lists the results for meshed networks. The FD-DSE and Newton DSE produce very similar SE results, since exact measurement constraints are used to calculate the power deviation over iterations. The FD-DSE gain matrix was enlarged by introducing additional variables ($P_{ij}, Q_{ij}, P_{ji}, Q_{ji}$). However, this matrix is very sparse, thus maintaining the efficiency of the FD-DSE. From Tables II and III, although the Newton-DSE uses fewer iterations, it requires more CPU time. This is because the gain matrix has to be reformulated and factorized at every iteration in the Newton-DSE, but is only needed during initialization for the FD-DSE. Since the branch current measurements are formulated as linear loss measurement functions, the results also show that FD-DSE does not need more iterations when these measurements are involved. From the results of Case 7, the proposed FD-DSE is more efficient than the Newton DSE for a large-scale system. Since the efficiency of a program also depends heavily on its coding techniques, the CPU times for these two methods listed in Table II are only for comparison under the same implementation conditions. From the results in Tables II and III, it can also be seen that the meshed network has little impact on the convergence of the proposed method. From the results for Cases 2 and 3 in Table III, the number of iterations for meshed networks is less than that for radial networks.

TABLE II
PERFORMANCE OF THE TWO DIFFERENT SE METHODS IMPLEMENTED ON A RADIAL NETWORK

Case	FD-DSE		Newton DSE		Maximum voltage deviation between FD-DSE and Newton DSE
	Iter.	CPU time(s)	Iter.	CPU time(s)	
1	7	0.0088	5	0.0338	6.25×10^{-6}
2	6	0.0093	5	0.0319	3.24×10^{-6}
3	7	0.0279	5	0.1123	3.79×10^{-6}
4	8	0.0481	5	0.2182	5.71×10^{-6}
5	8	0.0774	5	0.3535	5.66×10^{-6}
6	6	0.2680	5	0.9618	6.62×10^{-6}
7	7	3.3766	5	13.7085	9.49×10^{-6}

TABLE III
PERFORMANCE OF THE TWO DIFFERENT SE METHODS IMPLEMENTED ON A MESHED NETWORK

Case	FD-DSE		Newton DSE		Maximum voltage deviation between FD-DSE and Newton DSE
	Iter.	CPU time(s)	Iter.	CPU time(s)	
1	7	0.0151	5	0.0654	3.76×10^{-6}
2	5	0.0180	4	0.0617	5.89×10^{-6}
3	6	0.0355	5	0.1358	7.99×10^{-6}
4	7	0.0648	5	0.2843	4.11×10^{-6}
5	8	0.0924	5	0.4470	5.22×10^{-6}
6	7	0.3422	5	1.4683	4.19×10^{-6}
7	8	4.2965	5	20.4278	1.19×10^{-6}

B. Impact from Complex per unit Normalization

Complex per unit normalization is critical for implementing FD-DSE on a distribution network. From the results in Tables IV and V, complex per unit normalization improves the convergence of FD-DSE. Without complex per unit normalization, FD-DSE cannot converge within a limited number of iterations. From the results for Case 5 given in Tables IV and V under conventional p.u., after closing the tie lines in the 201-bus test feeder, the FD-DSE failed to converge in more than 20 iterations. The impedance parameters for tie lines are all identical, at 2.98257×10^{-9} + 2.98257×10^{-9}j p.u. These are small impedance branches compared to other branches with about 0.001–0.01 p.u. For FD-DSE under conventional p.u., small impedance branches have a greater impact on convergence, while for FD-DSE under complex p.u., small impedance branches have a smaller impact on convergence. It can be concluded that complex p.u. improves the numerical stability of FD-DSE.

TABLE IV
PERFORMANCE OF THE TWO DIFFERENT SE METHODS IMPLEMENTED ON A RADIAL NETWORK

case		FD-DSE with complex p.u.	FD-DSE with conventional p.u.
	ϕ_{base}	Iter.	Iter.

This article has been accepted for publication in a future issue of this journal, but has not been fully edited. Content may change prior to final publication. Citation information: DOI 10.1109/TSG.2017.2709463, IEEE Transactions on Smart Grid

1	1.524369	7	19
2	0.930988	6	11
3	0.455284	7	7
4	0.814445	8	7
5	0.965050	8	8
6	0.915803	6	10
7	0.917346	7	10

TABLE V
PERFORMANCE OF THE TWO DIFFERENT SE METHODS IMPLEMENTED ON A MESHED NETWORK

case	ϕ_{base}	FD-DSE with complex p.u. Iter.	FD-DSE with conventional p.u. Iter.
1	1.525099	7	18
2	0.922711	5	9
3	0.458971	6	9
4	0.811444	7	7
5	0.966187	8	> 20
6	0.860685	7	9
7	0.861821	8	13

C. Comparison with the Newton SE method using constant Jacobian matrix

Fast decoupled method is more robust than Newton Jacobian method with constant Jacobian under heavy load. Hence, to verify the performace of the proposed FD-DSE, the active and reactive power of load are increased to 1.3 times.

Table VI shows that Newton DSE with constant Jacobian is less efficient than proposed FD-DSE for a network with heavy load in all cases.

TABLE VI
PERFORMANCE OF THE FD-DSE METHODS AND NEWTON SE WITH CONSTANT JACOBIAN FOR A DISTRIBUTION NETWORK WITH HEAVY LOAD

Case	FD-DSE		Newton DSE with Constant Jacobian	
	Iter.	CPU time(s)	Iter.	CPU time(s)
1	7	0.0079	12	0.0141
2	7	0.0104	11	0.0173
3	7	0.0295	12	0.0978
4	8	0.0493	14	0.1163
5	8	0.0797	14	0.1539
6	7	0.2798	16	0.6756
7	7	3.4986	13	6.7732

D. Impact for SE with different BCCM configurations

In this section, test cases with a 69-bus distribution network with different BCCM configurations are conducted to demonstrate how BCCMs improve the estimation accuracy of FD-DSE.

The branch current measurement coverage rate η is defined as

$$\eta = \frac{n_{m-branch}}{n_{branch}} \tag{40}$$

where $n_{m-branch}$ is the number of BCCMs and n_{branch} is the total number of branches.

To characterize the estimation accuracy, the root mean square (RMS) of the estimation error for load power is defined as:

$$RMS_{load} = \sqrt{\frac{\sum\left|P_{load} - P_{load}^{se}\right|^2 + \sum\left|Q_{load} - Q_{load}^{se}\right|^2}{2n_{load}}} \tag{41}$$

where n_{Load} is the number of loads, P_{load} and Q_{load} are the original power flow results and P_{load}^{se} and Q_{load}^{se} are the state estimation results.

As shown in Table VI, when the BCCM coverage rate increases, the estimation accuracy is significantly improved. Hence, it is necessary to incorporate BCCMs into FD-DSE to obtain better estimation results.

TABLE VII
RESULTS OF FD-DSE WITH DIFFERENT NUMBERS OF BCCMS

η	RMS_{load}
0.1	2.19×10^{-2}
0.3	5.2×10^{-3}
0.6	2.8×10^{-3}
1	5.1×10^{-4}

E. Bad Data Analysis

Additional numerical tests are conducted on a 30-bus distribution network [26] as illustrated in Figure. 3. The test results are listed in Table VIII. The results show that FD-DSE incorporated with HTI can successfully identify multiple branch current magnitude measurements' errors and other types of measurements.

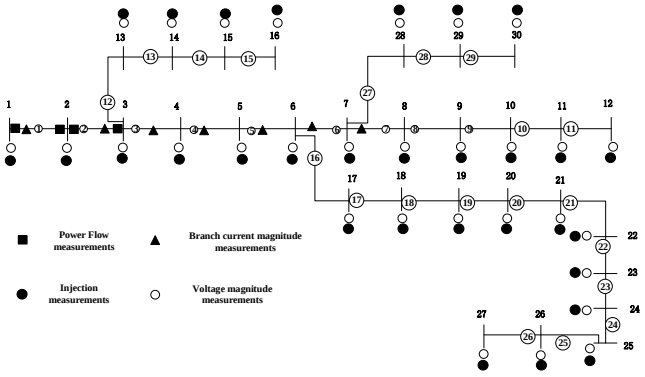

Figure 3 30-bus distribution network with various measurements

TABLE VIII
BAD DATA ANALYSIS

Error measurements	Identification results
Branch current magnitude measurements at branch 1-2	Errors are all identified
Branch current magnitude measurements	Errors are all

at branch 1-2 and branch 3-4	identified
Branch current magnitude measurements at branch 3-4 and branch 4-5	Errors are all identified
Power Flow measurements at branch 1-2	Errors are all identified
Power Flow measurements at branch 1-2 and Branch current magnitude measurements at branch 3-4	Errors are all identified

VII. CONCLUSION

In this study, branch ampere measurements were formulated as linear loss measurement functions, and a fast decoupled SE solution was developed for distribution networks based on complex per unit normalization. In this method, the Jacobian matrices are constant and convergence is maintained for distribution networks of different scales. The high efficiency of the proposed SE method is suitable for large scale distribution networks with ampere measurements.

The proposed method can be applied in high and medium voltage distribution networks, in which three-phase imbalance is not critical. To apply the method to low voltage distribution networks, which are always currently unobservable, this FD-DSE model should be expanded to a three-phase model with some approximations, which require further investigation. For unbalanced three-phase distribution systems, three-phase fast decoupled pattern can be tried in complex per unit system with assumption $\theta_a - \theta_b \approx 120^0$ etc. The detail of three-phase fast decoupled model can refer to [34].

REFERENCES

[1] F. C. Schweppe and J. Wildes, "Power System Static-State Estimation, Part I: Exact Model," *IEEE Transactions on Power Apparatus and Systems*, vol. PAS-89, no. 1, pp. 120–125, Jan. 1970.

[2] A. Primadianto and C. N. Lu, "A Review on Distribution System State Estimation," *IEEE Transactions on Power Systems*, vol. PP, no. 99, pp. 1–1, 2016.

[3] M. E. Baran and A. W. Kelley, "State estimation for real-time monitoring of distribution systems," *IEEE Transactions on Power Systems*, vol. 9, no. 3, pp. 1601–1609, Aug. 1994.

[4] K. I. Geisler, "Ampere Magnitude Line Measurements for Power Systems State Estimation," *IEEE Transactions on Power Apparatus and Systems*, vol. PAS-103, no. 8, pp. 1962–1969, Aug. 1984.

[5] A. Abur and A. G. Exposito, "Detecting multiple solutions in state estimation in the presence of current magnitude measurements," *IEEE Transactions on Power Systems*, vol. 12, no. 1, pp. 370–375, Feb. 1997.

[6] C. N. Lu, J. H. Teng, and W. H. E. Liu, "Distribution system state estimation," *IEEE Transactions on Power Systems*, vol. 10, no. 1, pp. 229–240, Feb. 1995.

[7] H. Wang and N. N. Schulz, "A revised branch current-based distribution system state estimation algorithm and meter placement impact," *IEEE Transactions on Power Systems*, vol. 19, no. 1, pp. 207–213, Feb. 2004.

[8] W. Wu, Y. Ju, B. Zhang, and H. Sun, "A distribution system state estimator accommodating large number of ampere measurements," *International Journal of Electrical Power & Energy Systems*, vol. 43, no. 1, pp. 839–848, 2012.

[9] A. Garcia, A. Monticelli, and P. Abreu, "Fast Decoupled State Estimation and Bad Data Processing," *IEEE Transactions on Power Apparatus and Systems*, vol. PAS-98, no. 5, pp. 1645–1652, 1979.

[10] J. J. Allemong, L. Radu, and A. M. Sasson, "A Fast and Reliable State Estimation Algorithm for AEP's New Control Center," *IEEE Transactions on Power Apparatus and Systems*, vol. PAS-101, no. 4, pp. 933–944, Apr. 1982.

[11] L. S. VanSlyck and J. J. Allemong, "Operating experience with the AEP state estimator," *IEEE Transactions on Power Systems*, vol. 3, no. 2, pp. 521–528, May 1988.

[12] R. R. Nucera and M. L. Gilles, "A blocked sparse matrix formulation for the solution of equality-constrained state estimation," *IEEE Transactions on Power Systems*, vol. 6, no. 1, pp. 214–224, Feb. 1991.

[13] A. Monticelli, C. A. F. Murari, and F. F. Wu, "A Hybrid State Estimator: Solving Normal Equations By Orthogonal Transformations," *IEEE Transactions on Power Apparatus and Systems*, vol. PAS-104, no. 12, pp. 3460–3468, Dec. 1985.

[14] L. Holten, A. Gjelsvik, S. Aam, F. F. Wu, and W. H. E. Liu, "Comparison of different methods for state estimation," *IEEE Transactions on Power Systems*, vol. 3, no. 4, pp. 1798–1806, Nov. 1988.

[15] K. A. Clements, G. W. Woodzell, and R. C. Burchett, "A new method for solving equality-constrained power system static-state estimation," *IEEE Transactions on Power Systems*, vol. 5, no. 4, pp. 1260–1266, Nov. 1990.

[16] A. Gjelsvik, S. Aam, and L. Holten, "Hachtel's Augmented Matrix Method - A Rapid Method Improving Numerical Stability in Power System Static State Estimation," *IEEE Transactions on Power Apparatus and Systems*, vol. PAS-104, no. 11, pp. 2987–2993, Nov. 1985.

[17] J. W. Wang and V. H. Quintana, "A Decoupled Orthogonal Row Processing Algorithm for Power System State Estimation," *IEEE Transactions on Power Apparatus and Systems*, vol. PAS-103, no. 8, pp. 2337–2344, Aug. 1984.

[18] F. Zhuang and R. Balasubramanian, "A Transformation-Decoupled Estimator for Power System State Estimation," *IEEE Transactions on Power Apparatus and Systems*, vol. PAS-104, no. 7, pp. 1738–1744, Jul. 1985.

[19] A. Monticelli and A. Garcia, "Fast decoupled state estimators," *IEEE Transactions on Power Systems*, vol. 5, no. 2, pp. 556–564, May 1990.

[20] L. Roy and T. A. Mohammed, "Fast super decoupled state estimator for power systems," *IEEE Transactions on Power Systems*, vol. 12, no. 4, pp. 1597–1603, Nov. 1997.

[21] O. L. Tortelli, E. M. Lourenco, A. V. Garcia, and B. C. Pal, "Fast Decoupled Power Flow to Emerging Distribution Systems via Complex pu Normalization," *IEEE Transactions on Power Systems*, vol. 30, no. 3, pp. 1351–1358, May 2015.

[22] B. Stott and D. Alsac, "Fast decoupled load flow," *IEEE Transcations on PAS*, pp. 859–867, 1974.

[23] A. Abur and A. G. Exposito, *Power System State Estimation:theory and implementation*. Boston: Marcel Dekker,Inc, 2004.

[24] I. S. Duff and J. Koster, "The design and use of algorithms for permuting large entries to the diagonal of sparse matrices," *Siam Journal on Matrix Analysis & Applications*, vol. 20, no. 4, pp. 889–901, 1999.

[25] N. P. Group, "REDS: REpository of Distribution Systems." http://www.dejazzer.com/reds.html, 2016.

[26] U. Eminoglu and M. H. Hocaoglu, "A new power flow method for radial distribution systems including voltage dependent load models," *Electric Power Systems Research*, vol. 76, no. 1–3, pp. 106–114, 2005.

[27] M. E. Baran and F. F. Wu, "Network reconfiguration in distribution systems for loss reduction and load balancing," *IEEE Transactions on Power Delivery*, vol. 4, no. 2, pp. 1401–1407, Apr. 1989.

[28] C.-T. Su, C.-F. Chang, and J.-P. Chiou, "Distribution network reconfiguration for loss reduction by ant colony search algorithm," *Electric Power Systems Research*, vol. 75, no. 2–3, pp. 190–199, 2005.

[29] C. Sanderson and R. Curtin, "Armadillo: a template-based C++ library for linear algebra," *Journal of Open Source Software*, vol. 1, p. 26, 2016.

[30] G. Guennebaud, B. Jacob, and others, "Eigen v3." 2010.

[31] X. S. Li, "An Overview of SuperLU: Algorithms, Implementation, and User Interface," *toms*, vol. 31, no. 3, pp. 302–325, Sep. 2005.

[32] A. Monticellli and A. Garcia, "Reliable Bad Data Processing for Real Time State Estimation", *IEEE Trans, on Power Apparatus and Systems*, Vol.PAS-102, No.3, pp.1126-1139, 1983

[33] L. Mili, Th Van Cutsem and M. Ribbens-Pavella, "Hypothesis Testing Identification: A New Method for Bad Data Analysis in Power System State Estimation", *IEEE Trans, on Power Apparatus and Systems*, Vol.PAS-103, No.11, pp.3239-3252, 1984

[34] R. K. Portelinha and O. L. Tortelli ,"Three phase fast decoupled power flow for emerging Distribution Systems", *2015 IEEE PES Innovative Smart Grid Technologies Latin America* (ISGT LATAM), 81-86, 2015.

[35] B. M. Zhang and K. L. Lo, "A Recursive Measurement Error Estimation Identification Method for Bad Data Analysis in Power System State Estimation", *IEEE Trans. on Power Systems*,Vol. PWRS-6, No. 1, 1991, pp. 191-197 0885-8950.

This article has been accepted for publication in a future issue of this journal, but has not been fully edited. Content may change prior to final publication. Citation information: DOI 10.1109/TSG.2017.2709463, IEEE Transactions on Smart Grid

VIII. BIOGRAPHIES

Yuntao Ju (M'13) received his B.Sc in mechanical engineering in 2008 and his Ph.D. degree in electrical engineering in 2013, all from Tsinghua University. He was an awardee of excellent graduates from Tsinghua University in 2008. In November 2013, He has been a visiting scholar to University of Toronto for a year. In 2015, Dr. Yuntao Ju joined china electric power research institute as a research fellow. He is now an associate professor in College of Information and Electrical Engineering, China Agricultural University (CAU), Beijing, P R China. His research interests include hybrid energy system modeling, high speed dynamic simulation, large scale system parameter identification, state estimation and uncertainty optimization..

Wenchuan Wu (SM'14) received the B.S., M.S., and Ph.D. degrees from the Electrical Engineering Department, Tsinghua University, Beijing, China. He is currently a Professor in the Department of Electrical Engineering of Tsinghua University. His research interests include Energy Management System, active distribution system operation and control, and EMTP-TSA hybrid real-time simulation.

Prof. Wu is an *IET Fellow*, associate editor of *IET Generation, Transmission & Distribution*, *Electric Power Components and Systems*.

Fuchao Ge received the Bachelor Degree of Engineering in electrical engineering from Linyi University, Linyi, China, in 2014. Now he is pursuring master degree of China Agricultural University, his research interests include Power system state estimation, parameter identification and electricity market.

Kang Ma is working as a lecturer at University of Bath. His research focuses on three-phase unbalanced low voltage networks. He worked as an R&D engineer at China Electric Power Research Institute (Beijing) from 2011 to 2014, during which time he developed the first version of the reliability assessment module for a distribution network planning platform. This platform has been widely applied to over 20 provincial grid companies in China. He received his PhD degree in Electrical Engineering from the University of Manchester (U.K.) and his B.Eng. degree from Tsinghua University (China).

Yi Lin is an engineer with Electric Power Research Institute of Fujian Electric Power Limited Company. His research interests include distribution network planning and operation.

Lin Ye (M'98,SM'04) received his B.Sc. from WuHan University, P R China in 1992 and his Ph.D. degree in 2000 from the Institute of Electrical Engineering (IEE), Chinese Academy of Sciences (CAS), all in electrical engineering. He has been pursuing research at ForschungsZentrum Karlsruhe(FZK) (*now merged with University of Karlsruhe(TH) to form Karlsruhe Institute for Technology, KIT) as a research fellow of Alexander von Humboldt Stiftung/Foundation (AvH) of Germany from 2000 to 2002. In 2004, Dr. Lin Ye joined the Interdisciplinary Research Center (IRC), Department of Engineering/Cavendish Laboratory, the University of Cambridge, United Kingdom, as a research fellow. At Cambridge Laboratory, he had been involved in developing a novel resistive type of fault current limiter prototype for electrical marine propulsion which was funded by Rolls-Royce Plc and the Department of Trade & Industry (DTI) of the United Kingdom.

He is currently a full professor in electrical power engineering at the Department of Electric Power Systems, China Agricultural University (CAU), Beijing, P R China. His research interests are in the areas of electrical power system analysis & control, power grid modeling & simulation, renewable energy generation & system integration and dispatching as well as wind/solar power forecasting.